

# Straightforward and accurate automatic auxiliary basis set generation for molecular calculations with atomic orbital basis sets

Susi Lehtola\*

*Molecular Sciences Software Institute, Blacksburg, Virginia 24061, United States*

E-mail: susi.lehtola@alumni.helsinki.fi

## Abstract

Density fitting (DF), also known as the resolution of the identity (RI), is a widely used technique in quantum chemical calculations with various types of atomic basis sets—Gaussian-type orbitals, Slater-type orbitals, as well as numerical atomic orbitals—to speed up density functional, Hartree–Fock, and post-Hartree–Fock calculations. Traditionally, custom auxiliary basis sets are hand-optimized for each orbital basis set; however, some automatic schemes have also been suggested. In this work, we propose a simple yet numerically stable automated scheme for forming auxiliary basis sets with the help of a pivoted Cholesky decomposition, which is applicable to any type of atomic basis function. We exemplify the scheme with proof-of-concept calculations with Gaussian basis sets and show that the proposed approach leads to negligible DF/RI errors in Hartree–Fock (HF) and second-order Møller–Plesset (MP2) total energies of the non-multireference part of the W4-17 test set when used with orbital basis sets of at least polarized triple- $\zeta$  quality. The results are promising for future applications employing Slater-type orbitals or numerical atomic orbitals, as well as schemes based on the use of local fitting approaches. Global fitting approaches can also be used, in which case the

high-angular-momentum functions produced by the present scheme can be truncated to minimize the computational cost.

# 1 Introduction

Density fitting (DF),<sup>1-5</sup> also known as the resolution of the identity (RI),<sup>6</sup> is a pivotal technique in several recently developed computational approaches for electronic structure theory. In the DF/RI approach, two-electron integrals are expressed in terms of an auxiliary basis set in Mulliken notation as<sup>6</sup>

$$(\mu\nu|\sigma\rho) \approx \sum_{AB} (\mu\nu|A)(A|B)^{-1}(B|\sigma\rho), \quad (1)$$

where  $\mu$ ,  $\nu$ ,  $\sigma$ , and  $\rho$  are orbital basis functions,  $A$  and  $B$  are auxiliary basis functions, and  $(A|B)^{-1}$  denotes the  $AB$  element of the inverse of the Coulomb overlap matrix. The key of the DF/RI approach is that the set of atomic orbital (AO) products  $\mu\nu$  is heavily linearly dependent, and can be accurately approximated with only a linearly scaling number of auxiliary functions  $A$ .

Another key feature behind the usefulness of the DF/RI approach is that the two-electron integrals in equation (1) factorize. This factorization can be exploited in many applications, as it allows the optimization of the order of various contractions. For instance, the Coulomb matrix

$$J_{\mu\nu} = \sum_{\rho\sigma} (\mu\nu|\sigma\rho)P_{\sigma\rho}, \quad (2)$$

where  $\mathbf{P}$  denotes the density matrix, can be efficiently evaluated with RI—yielding the RI-J scheme—in three steps:<sup>7</sup> determination of the bare expansion coefficients  $\gamma_B = \sum_{\rho\sigma} (B|\rho\sigma)P_{\sigma\rho}$ , projection into the orthonormal basis  $\tilde{\gamma}_A = \sum_B (A|B)^{-1}\gamma_B$ , and assembly of the Coulomb matrix  $J_{\mu\nu} = \sum_A (\mu\nu|A)\tilde{\gamma}_A$ . Exchange matrices  $\mathbf{K}_\sigma$  are also often formed with RI; the resulting RI-K algorithm is somewhat more complicated than RI-J but efficient implementations

have been developed also for this case.<sup>8,9</sup>

More generally, the transformation from the AO basis to the molecular orbital (MO) basis that arises in various post-Hartree–Fock theories

$$(pq|rs) = \sum_{\mu\nu\sigma\rho} C_{\mu p} C_{\nu q} C_{\sigma r} C_{\rho s} (\mu\nu|\sigma\rho), \quad (3)$$

where  $\mathbf{C}$  is the matrix of MO coefficients, scales as  $\mathcal{O}(N^5)$  with the exact integrals  $(\mu\nu|\sigma\rho)$  while the DF variant only scales as  $\mathcal{O}(N^3)$ , with  $N$  denoting the number of AO basis functions. DF thus yields significant speedups for calculations employing second-order Møller–Plesset perturbation theory (MP2),<sup>10,11</sup> for instance. DF/RI is especially useful when the orbital basis set is large, because the calculation of the exact two-electron integrals as well as the integral transforms become slow in such cases.

Although most Gaussian-basis programs that support DF also also support the use of exact two-electron integrals, there are also programs that do not support exact integrals. For instance, the BAGEL program<sup>12</sup> relies exclusively on DF in all calculations, as the DF integrals can be kept in memory on modern hardware, and as the speedups DF offers often have negligible effect on the accuracy of the calculation.<sup>12</sup> For similar reasons, DF is the default mode of operation in the Gaussian-basis PSI4 program,<sup>13</sup> as well, even though PSI4 also supports the use of exact two-electron integrals.

Another important application of DF techniques can be found in quantum chemistry programs employing atomic orbital basis sets other than Gaussian-type orbitals, as the molecular two-electron integrals are famously difficult to compute in such cases. Molecular calculations with exact exchange as well as calculations at post-Hartree–Fock levels of theory are made tractable by DF in combination with any type of atomic orbital basis set, because the Coulomb potential of the auxiliary functions is easy to evaluate numerically,<sup>14</sup> leaving only a three-dimensional integral which can be evaluated by quadrature with Becke’s multicenter method,<sup>15</sup> for instance. Examples of such an approach are the Slater-type orbital

ADF program,<sup>16</sup> as well as the numerical atomic orbital FHI-AIMS program.<sup>17</sup>

A central aspect of RI is the need for an auxiliary basis set. Traditionally, an auxiliary basis set is optimized for each orbital basis set with painstaking electronic structure calculations on a set of sample systems.<sup>18</sup> For RI-J and RI-K, universal auxiliary basis sets by Weigend<sup>19,20</sup> are typically used, even though the sets are formally tailored only for the Karlsruhe def2 basis sets<sup>21</sup> that reach up to polarized quadruple- $\zeta$  quality. Post-Hartree–Fock calculations in turn typically employ orbital-basis-specific auxiliary basis sets parametrized by various authors.<sup>11,22–25</sup> Similarly, the Slater-type orbital basis sets used in ADF employ tailored fitting basis sets.<sup>26,27</sup>

Although standard orbital and auxiliary basis sets are immensely useful for several kinds of applications, they are not cost-efficient for the reproduction of properties that are sensitive to aspects of the wave function which do not have a significant impact on the total energy. For instance, an accurate modeling of nuclear magnetic properties requires specialized Gaussian basis sets with extremely tight exponents,<sup>28,29</sup> auxiliary basis sets for which may not be readily available. Another example can be found in electron momentum densities which are sensitive to the diffuse part of the wave function.<sup>30</sup> While specialized basis sets have likewise been developed for this purpose,<sup>31,32</sup> they lack corresponding auxiliary basis sets. Yet another examples are basis sets meant for core excitation spectroscopies,<sup>33</sup> as well as the near-complete-basis-set-limit Gaussian basis sets for the whole periodic table from H to Og formed from first principles,<sup>34</sup> which similarly lack tailored auxiliary basis sets.

Automatic schemes for generating auxiliary basis sets from an orbital basis set are thus immensely useful in many applications. Yang et al.<sup>35</sup> proposed an algorithm for forming RI-J fitting sets from Gaussian orbital basis sets by grouping together similar exponents arising from all possible basis function products. Stoychev et al.<sup>36</sup> proposed a heuristic algorithm that forms reasonably compact Gaussian auxiliary basis sets that should be suitable for calculations both at the self-consistent field<sup>37</sup> and post-Hartree–Fock levels of theory. However, the schemes of Yang et al. and Stoychev et al. have a number of adjustable parameters and

are therefore not completely black-box algorithms; moreover, they are limited to the use of a Gaussian basis set.

Automatic algorithms are especially useful when they can be used with any type of atomic basis set. Ren et al.<sup>17</sup> suggested an approach where a Gram–Schmidt procedure is used to choose a linearly independent set of basis function products as the auxiliary basis. The algorithm of Ren et al. is in principle applicable to any type of atomic basis set; their implementation in the FHI-AIMS program<sup>38</sup> uses numerical atomic orbitals (see ref. 14 for discussion on various atomic basis functions). However, the Gram–Schmidt procedure used by Ren et al. is not guaranteed to process the auxiliary function candidates in an optimal order, and thereby requires the use of an additional numerical threshold for discarding functions that can be described sufficiently well with the auxiliary radial functions previously included by the procedure. Still, when applied to calculations with numerical atomic orbital representations of standard Gaussian basis sets,<sup>14</sup> the procedure of Ren et al. has been found to afford sub-meV-level RI errors in HF and MP2 total energies.<sup>17,39</sup>

Aquilante et al.<sup>40,41</sup> pioneered an approach for forming auxiliary basis sets with a Cholesky decomposition of the two-electron integral tensor.<sup>42</sup> Their algorithm is controlled by a single parameter: the Cholesky decomposition threshold. Boström et al.<sup>43</sup> showed that the auxiliary sets from this approach can be made exact, that is, the DF calculations can be made to agree with ones employing exact two-electron integrals when the decomposition threshold is sufficiently small. However, this approach that is implemented in the OPENMOLCAS program<sup>44</sup> employs mixtures of Cartesian and spherical basis functions as the auxiliary basis set even when the orbital basis only has spherical functions,<sup>45</sup> thereby requiring a complicated approach which is not supported in most quantum chemistry codes. Moreover, it turns out that unreliable results are obtained if the mixed-form basis is used in either pure Cartesian or pure spherical form, the latter being the standard choice especially in the case of auxiliary basis sets. An automated algorithm that produces spherical fitting functions would thus be highly useful.

In this work, we suggest a simplified approach for forming auxiliary basis sets, which is a straightforward extension of the method developed in refs. 46 and 47 for solving issues with overcomplete orbital basis sets. Like the scheme of Aquilante et al.<sup>41</sup>, the present algorithm produces auxiliary basis sets that can be argued to be optimal; however, unlike the scheme of Aquilante et al. the present sets employ only spherical functions. At further variance to the scheme of Aquilante et al., which requires access to the full two-electron integrals  $(\mu\nu|\rho\sigma)$ , the basic version of the present approach only requires two-index integrals  $(A|B)$  like the scheme of Ren et al.<sup>17</sup> Our basic scheme is obtained from the Ren et al.<sup>17</sup> scheme by replacing the Gram–Schmidt method by the pivoted Cholesky method, which is a numerically stable way to find an optimal set of auxiliary functions.<sup>46,48</sup> However, as we will show in this work, the present scheme can also be combined with the Cholesky decomposition of the two-electron integrals tensor  $(\mu\nu|\rho\sigma)$ , resulting in more cost-efficient auxiliary basis sets.

The layout of the manuscript is the following. In section 2, we discuss the full theory behind the present approach. We describe the implementation of the method in section 3, and describe the computational methods used in this work in section 4. The accuracy of the present method for RI-HF and RI-MP2 calculations of total energies of the W4-17 test set of molecules<sup>49</sup> is demonstrated in section 5; representative timings on commodity hardware as well as further details of the algorithm are also discussed. The article concludes in a summary and discussion in section 6.

## 2 Theory

Mulliken notation defines the electron repulsion integrals as

$$(\mu\nu|\rho\sigma) = \int \frac{\chi_\mu(\mathbf{r})\chi_\nu(\mathbf{r})\chi_\rho(\mathbf{r}')\chi_\sigma(\mathbf{r}')}{|\mathbf{r} - \mathbf{r}'|} d^3r d^3r', \quad (4)$$

where the basis functions have been assumed to be real. In this work, both the orbital and the auxiliary basis functions are assumed to be atomic

$$\chi_\mu(\mathbf{r}) = R_\mu(r)Y_{l_\mu}^{m_\mu}(\hat{\mathbf{r}}), \quad (5)$$

where  $R_\mu(r)$  is the radial function, and  $Y_l^m$  are real-valued spherical harmonics. In order for equation (1) to be accurate, it is seen from equation (4) that the auxiliary basis set  $\{A\}$  should be able to represent all orbital basis function products  $\{\chi_\mu\chi_\nu\}$  accurately; or, to be more precise, the potentials of  $\{A\}$  should be able to represent all the potentials of  $\{\chi_\mu\chi_\nu\}$ . As the set  $\{\chi_\mu\chi_\nu\}$  is heavily linearly dependent, one should pick out the product functions in a way that spans all possible degrees of freedom in the set as quickly as possible. This is exactly what can be accomplished with a pivoted Cholesky decomposition.

The present approach to form auxiliary basis sets is thus the following. The first step is to form all basis function products  $\mu\nu$ , yielding the set of candidate auxiliary functions  $\{\tilde{A}\}$ . The products are of the form  $R_{\mu\nu}(r)Y_L^M(\hat{\mathbf{r}})$ , where  $R_{\mu\nu}(r) = R_\mu(r)R_\nu(r)$  is a product of the radial basis functions, while the angular part may be coupled to

$$|l_\mu - l_\nu| \leq L \leq l_\mu + l_\nu \quad (6)$$

and  $M = m_\mu + m_\nu$ . Note that in this work, spherical auxiliary functions are always used, as is the standard approach.<sup>7</sup> Moreover, the present algorithm is shell-driven, that is, the auxiliary functions are always handled one complete shell of functions ( $M = -L, \dots, L$ ) at a time.

In the second step, the candidate functions' Coulomb overlap matrix

$$S_{\tilde{A}\tilde{B}} = (\tilde{A}|\tilde{B}). \quad (7)$$

is formed. The key point here is that the matrix  $S_{\tilde{A}\tilde{B}}$  is block-diagonal in the angular momen-

tum (see Appendix I): the dependence on the magnetic quantum number  $M$  can be omitted (justifying the shell-based approach), leaving only dependence on the azimuthal quantum number  $L$ . We can then form the matrix  $S_{\tilde{A}\tilde{B}}$  separately for each angular momentum  $L$  of the auxiliary basis set, and the matrix elements only depend on the radial functions  $\tilde{A}$  and  $\tilde{B}$ . As shown in Appendix I, the matrix elements in equation (7) have a trivial analytic form for Gaussian and Slater type orbitals, whereas the integrals can be evaluated by quadrature when other kinds of atomic basis functions such as numerical atomic orbitals are used.<sup>14,50</sup>

Third, the method of refs. 46 and 47 is used to pick a set of auxiliary functions  $A$  from the pool  $\tilde{A}$ . Since all basis function products  $\mu\nu$  are included in the pool  $\tilde{A}$ , and the procedure ensures that all  $\tilde{A}$  are expressible in the basis  $A$ , since the residual norm of  $\mathbf{S}$  is small after the Cholesky decomposition,<sup>46</sup> the procedure yields an accurate auxiliary basis that is optimal.<sup>46,48</sup> The mathematical reasoning for the optimality is the following. The Cholesky decomposition is given by<sup>51</sup>

$$S_{\mu\nu} \approx \sum_P L_{\mu P} L_{\nu P}. \quad (8)$$

The pivoted algorithm, which is discussed extensively in ref. 48, proceeds by iteratively adding new columns in  $\mathbf{L}$  in an optimal order. The pivot—the function to add—is the function  $A$  with the largest diagonal remainder,  $(\mathbf{S} - \mathbf{L}\mathbf{L}^T)_{AA}$ . This means that at every iteration, the pivoting procedure adds the candidate function that is worst described by the set of the previous pivot functions, until the predefined convergence threshold is reached. Exactly this feature of the pivoted Cholesky algorithm is the reason for its quick convergence,<sup>48</sup> affording the optimal molecular basis sets pursued in refs. 46 and 47, as well as the optimal auxiliary basis sets pursued in this work.

Because auxiliary functions are normalized,  $(\tilde{A}|\tilde{A}) = 1$ ,  $\mathbf{S}$  has a unit diagonal as in the case of the usual overlap matrix discussed in ref. 46. Because of the unit diagonal, the pivoted Cholesky algorithm starts out with no information on the relative importance of the candidate basis functions. The procedure of ref. 46 solved this issue by presorting the basis functions by spatial extent, so that the functions with the smallest spatial extent—which



typically do not cause problems with linear dependencies—are processed first. After the first iterations, the diagonal remainders no longer equal unity, thus unleashing the full power of the pivoted Cholesky algorithm.

However, ordering the functions by spatial extent is not the most elegant solution in applications to the calculation of strongly repulsive internuclear potentials, for example. In this application, the internuclear distance can be small enough to cause overcompleteness even for the tightest basis functions that represent core orbitals. A better solution that requires only the overlap matrix  $\mathbf{S}$  can be motivated by the Gershgorin circle theorem.<sup>52</sup>

Per the note in ref. 47, we sort the rows and columns of  $\mathbf{S}$  in increasing off-diagonal norm  $S_{\bar{A}} = \sum_B |S_{\bar{A}\bar{B}}|$ . This guarantees that the functions are fed into the pivoted Cholesky procedure in an increasing order of potential linear dependencies. The pivoted Cholesky is then initialized with the most independent basis functions, which should anyway be included in the basis. This should result in an optimal order in the pivoted Cholesky decomposition, and result in the smallest possible subsets of basis functions chosen by the pivoted Cholesky algorithm. This procedure also makes the pivoted Cholesky algorithm self-sufficient, as in contrast of the original approach used in refs. 46 and 47, all the necessary information can be extracted from the decomposed matrix, itself. In molecular applications along the lines of refs. 46 and 47, this ordering also accounts for geometric effects: the basis functions that have the least overlap with functions on other centers are processed first.

In the basic formalism, the present scheme only requires the computation of the two-index integrals in equation (7). Alternatively, the present method can also be combined with the Cholesky decomposition of the electron repulsion integrals, in the lines of Aquilante et al.<sup>40,41</sup> Instead of forming the pool of candidate auxiliary functions  $\{\tilde{A}\}$  by generating *all* products of basis functions in step 1, one can instead include only those shell products that are chosen by the pivoted Cholesky decomposition of the full atomic two-electron integrals tensor<sup>42,53</sup>

$$(\mu\nu|\rho\sigma) \approx \sum_P L_{\mu\nu}^P L_{\rho\sigma}^P; \quad (9)$$

note the similarity of equations (1) and (9) which is the motivation for the approach of Aquilante et al<sup>40,41</sup> as well as the present approach. For each pivot index  $\mu\nu$  chosen by the decomposition, the product of the shells that the orbital basis functions  $\mu$  and  $\nu$  belong to is added to the list of candidate shells.

Using the Cholesky decomposition of the two-electron integrals to choose the pool of candidate functions in step 1 leads to smaller auxiliary basis sets than using all possible atomic-orbital products as candidates, as will be shown later in this work. The difference is especially noticeable for high-angular-momentum orbital basis sets. For this reason, we will call these auxiliary basis sets *reduced auxiliary basis sets*, whereas the auxiliary basis sets formed from the consideration of all possible product functions are termed *full auxiliary basis sets*.

Although, in principle, different thresholds could be used for the pivoted Cholesky decomposition of the two-electron integral tensor and the pivoted Cholesky decomposition of the candidate auxiliary basis functions' Coulomb overlap matrix (equation (7)) which is used to choose the auxiliary basis functions in this work, for simplicity we have opted to use the same threshold  $\tau$  for both, as thresholds of  $\tau = 10^{-3}$  to  $\tau = 10^{-7}$  are reasonable for either part of the problem. Decreasing the threshold  $\tau$  then simultaneously results in more candidate functions from the decomposition of the two-electron integrals tensor, as well as a tighter criterion for the representation of all of the candidate functions by the chosen auxiliary basis set.

### 3 Implementation

Both the full and the reduced variants of the present approach were implemented for Gaussian basis sets in ERKALE<sup>54,55</sup> by building on top of the existing implementation<sup>56</sup> of the Cholesky decomposition of two-electron integrals for molecular calculations.<sup>42,53</sup> For clarity, the present scheme for forming auxiliary basis sets discussed in section 2 is summarized in

algorithm 1; details of the algorithm that are specific to the present use of Gaussian basis sets will be discussed below. For comparison, the AutoAbs and AutoAux methods of Yang et al.<sup>35</sup> and Stoychev et al.<sup>36</sup>, respectively, were implemented in the Python backend library of the Basis Set Exchange<sup>57</sup> as part of this work.

The use of Gaussian basis sets implies some limitations in the present proof-of-concept study, which need to be documented. First, we will only consider fully uncontracted orbital basis sets in the construction of the auxiliary basis, as this makes the algorithm simpler; this means that the orbital basis set is always decontracted before building the auxiliary basis set. (Note that applications to numerical atomic orbitals will not require such a step, because the product of radial functions  $R_{\mu\nu}(r) = R_\mu(r)R_\nu(r)$  is simply a new numerical atomic orbital, although potential issues with aliasing<sup>14</sup> should be kept in mind.)

Second, Gaussian-type orbitals have a fixed radial form

$$R_{nl}^{\text{GTO}}(r) = r^l \exp(-\alpha_{nl}r^2) \quad (10)$$

which needs to be considered in the assembly of the pool of candidate functions. The product of two Gaussian radial functions

$$R_\mu(r)R_\nu(r) = r^{l_\mu+l_\nu} e^{-(\alpha_\mu+\alpha_\nu)r^2} \quad (11)$$

spawns candidates to multiple angular momentum channels  $L$  according to equation (6); each candidate has the form of equation (10). For example, an F function ( $l = 3$ ) with exponent  $\alpha$  can couple with itself to  $0 \leq L \leq 6$ . While the real product radial function is  $r^6 \exp(-2\alpha r^2)$ , the form of the actual auxiliary functions  $r^L \exp(-2\alpha r^2)$  depends on the value of the coupled angular momentum  $L$ . The real product function is more diffuse than the candidate for  $L \leq \max L$ ; this difference has to be captured by the algorithm. Following Stoychev et al.<sup>36</sup>, we solve this issue by employing an effective exponent  $\alpha_L$  for the candidate function  $r^L \exp(-2\alpha_L r^2)$  so that the expectation value of  $\langle r \rangle$  for the generated auxiliary

function candidate agrees with the expectation value of  $\langle r \rangle$  computed with the true radial product function; this procedure is documented in Appendix II.

## 4 Computational Methods

As was already mentioned in the Introduction, the W4-17 database of molecules<sup>49</sup> is used to test the auxiliary basis sets. RI-HF and RI-MP2 calculations were performed with the double- $\zeta$  (2ZaPa-NR) to quintuple- $\zeta$  (5ZaPa-NR) orbital basis sets of Ranasinghe and Petersson<sup>58</sup> using PSI4.<sup>13</sup> The orbital basis sets and the corresponding AutoAux sets were obtained from the Basis Set Exchange.<sup>57</sup> Conventional HF and MP2 calculations were carried out with GAUSSIAN'09;<sup>59</sup> manipulations to the input basis were disabled with the setting IOp(3/60=-1). A basis set linear dependence threshold of  $10^{-7}$  was used in both programs; program defaults were used otherwise. To ensure the validity of RI-MP2, the multireference part of the database is excluded from the analysis, as is the hydrogen atom that has no correlation energy in RI-MP2 and for which the exchange and Coulomb terms cancel out in RI-HF. Core orbitals were frozen in all MP2 calculations.

## 5 Results

### 5.1 Full auxiliary basis versus reduced auxiliary basis

As was mentioned in section 2, the present approach can be implemented in two ways. The first is to pick the auxiliary basis set from the set of all possible orbital products (full approach); the second is to pick the auxiliary basis set from only the set of orbital products that are picked up by the Cholesky decomposition of the two-electron integral tensor (reduced approach). To illustrate the difference between these two approaches, the compositions of the auxiliary basis sets arising from the 2ZaPa-NR and 5ZaPa-NR orbital basis sets are shown in tables 1 and 2, respectively.

---

**Algorithm 1** Summary of the algorithm for forming the auxiliary basis starting from the orbital basis specified for an atom.

---

1. Obtain the orbital basis set defined by the radial functions  $R_{nl}(r)$  with angular momentum  $l$ ,  $\chi_\alpha = R_{n_\alpha l_\alpha}(r)Y_{l_\alpha}^{m_\alpha}(\mathbf{r})$ . Each radial function  $R_{nl}(r)$  thus corresponds to the  $2l + 1$  functions with  $m = -l, \dots, l$ .
2. Form all products of orbital basis functions  $\chi_\alpha \chi_\beta$ ; this yields the full set of candidate functions. The reduced set is obtained by considering only those products of basis functions that appear as pivot indices in the Cholesky decomposition of the two-electron integral tensor, instead.

The radial part of the basis function products is  $R_{n_\alpha l_\alpha}(r)R_{n_\beta l_\beta}(r)$ , and the angular part is  $Y_{l_\alpha}^{m_\alpha}(\mathbf{r})Y_{l_\beta}^{m_\beta}(\mathbf{r})$ . As the product of spherical harmonics is closed, the angular part can be rewritten in terms of spherical harmonics in the range  $|l_\alpha - l_\beta| \leq L \leq l_\alpha + l_\beta$ . The candidate auxiliary functions are then identified as  $R_{n_\alpha l_\alpha}(r)R_{n_\beta l_\beta}(r)Y_L^M$ .

If basis functions with a rigid analytic form are employed, like the even-tempered Gaussian functions of this work, the radial function products  $R_{n_\alpha l_\alpha}(r)R_{n_\beta l_\beta}(r)$  are replaced everywhere in the algorithm by an effective radial function  $R_{n_\alpha \beta L}(r)$  for each value of  $L$ , as discussed in Appendix II.

3. As Appendix I demonstrates, the Coulomb overlap matrix of the candidate functions is diagonal in  $L$ , meaning that all the candidate radial functions  $R_{n_\alpha l_\alpha}(r)R_{n_\beta l_\beta}(r)$  corresponding to a given final value of  $L$  can be considered together. Therefore, the auxiliary basis can be determined separately for each value of  $L$ :
    - (a) Form the Coulomb overlap matrix  $S_{\tilde{A}\tilde{B}} = (\tilde{A}|\tilde{B})$  for the candidate functions corresponding to the given  $L$  shell. Because the set of candidate functions is heavily overcomplete, this matrix is extremely ill-conditioned.
    - (b) Use the pivoted Cholesky decomposition of refs. 46 and 47 to choose a linearly independent set of auxiliary functions from the pool of candidate functions with the given  $L$ .
      - i. Order the candidate functions in increasing values of off-diagonal overlap,  $s_{\tilde{A}} = \sum_{\tilde{B} \neq \tilde{A}} |S_{\tilde{A}\tilde{B}}|$ . This guarantees that the most linearly independent candidate functions are picked first.<sup>47</sup>
      - ii. Perform the pivoted Cholesky decomposition<sup>48</sup> for the reordered Coulomb overlap matrix  $\mathbf{S}$  up to the specified decomposition threshold  $\tau$  with the LAPACK [Linear Algebra PACKage] routine `dpstrf()`, for example, and store the returned pivot indices.
      - iii. Map the pivot indices back to the original indexing of the candidate functions.
    - (c) Add the candidate radial functions corresponding to the used pivot indices to the auxiliary basis.
-

The data in table 1 suggest that the differences between the full and the reduced auxiliary basis sets are small for small orbital basis sets. In contrast, significant differences are observed in the case of large orbital basis sets exemplified by table 2.

Even though the compositions of the full and reduced auxiliary basis sets are similar at both small and large angular momentum, the differences at intermediate angular momentum are huge. For instance, the reduced auxiliary basis contains roughly just one half the number of f, g, and h functions of the full auxiliary basis. This difference between the two approaches is easy to understand. Products of high-angular momentum basis functions can couple to many values of angular momentum. For instance, the product of two F functions ( $l = 3$ ) may have components ranging from S functions to I functions ( $l = 6$ ). If the coupling coefficients are small at high angular momenta, the value of the two-electron integral may be dominated by contributions from the low-angular-momentum functions. The decomposition of the two-electron integrals tensor picks out only those basis function products that are necessary to describe the two-electron integrals, leading to the observed improvement in efficiency.

The accuracy of the full and reduced auxiliary basis sets can be quantified by comparing the resulting errors in the diagonal of the electron repulsion integral tensor  $(\mu\nu|\mu\nu)$  for which the error is negative definite:  $(\mu\nu|\mu\nu)$  is essentially the self-interaction energy of the electron density given by  $\chi_\mu(\mathbf{r})\chi_\nu(\mathbf{r})$ . The diagonal integral evaluated with RI using equation (1),  $(\widetilde{\mu\nu}|\widetilde{\mu\nu})$ , is smaller than the exact value; giving rise to an error metric

$$\Delta = \sum_{\mu\nu} \left[ (\mu\nu|\mu\nu) - (\widetilde{\mu\nu}|\widetilde{\mu\nu}) \right] \geq 0 \quad (12)$$

which we have implemented in ERKALE.<sup>54,55</sup>

Equation (12) can also be used to compare other types of auxiliary basis sets in a first-principles fashion. Such a comparison is shown in table 3 for the Fe def2-QZVP orbital basis set;<sup>60</sup> other choices for the orbital basis and other elements yield similar results. The comparison includes the universal auxiliary basis sets for RI-J<sup>19</sup> and RI-JK<sup>20</sup> calculations,

Table 1: Composition of 2ZaPa-NR and the resulting AutoAux basis as well as the full and reduced auxiliary basis sets with threshold  $\tau = 10^{-7}$ .

atom	primitive orbital basis	AutoAux basis	full auxiliary basis	reduced auxiliary basis
H	6s1p	12s2p2d	12s6p1d	10s6p1d
He	7s1p	10s2p2d	13s6p1d	11s6p1d
Li	9s5p1d	16s13p12d2f	22s21p16d5f1g	20s16p13d5f1g
Be	10s5p1d	16s13p12d2f	22s21p17d5f1g	21s17p14d5f1g
B	10s6p1d	16s13p12d2f	22s21p18d6f1g	21s19p15d6f1g
C	11s6p1d	16s13p12d2f	23s23p19d6f1g	22s19p15d6f1g
N	11s7p1d	16s13p12d2f	24s24p21d7f1g	23s21p16d6f1g
O	11s7p1d	16s13p12d2f	24s23p21d7f1g	23s22p16d7f1g
F	11s8p1d	16s13p12d2f	24s24p22d8f1g	23s22p18d7f1g
Ne	11s8p1d	16s13p13d2f	24s24p22d8f1g	23s22p18d7f1g
Na	14s9p2d	21s19p18d5f	31s31p28d16f3g	29s28p24d12f3g
Mg	15s9p2d	21s18p16d5f	31s31p26d16f3g	28s27p22d12f3g
Al	14s10p2d	20s17p16d5f	30s30p27d17f3g	30s28p23d12f3g
Si	14s10p2d	20s17p16d5f	29s30p27d17f3g	28s28p24d12f3g
P	14s10p2d	19s16p15d5f	29s29p27d17f3g	28s27p23d12f3g
S	14s10p2d	19s16p15d5f	29s29p27d17f3g	28s26p23d13f3g
Cl	14s10p2d	19s16p15d5f	29s29p27d17f3g	27s26p24d13f3g
Ar	14s10p2d	19s16p15d5f	29s29p27d16f3g	28s26p23d12f3g

the auxiliary basis set for MP2 calculations with the slightly larger def2-QZVPP orbital basis set,<sup>23</sup> as well as automatically generated auxiliary basis sets for the def2-QZVP orbital basis using the AutoAbs<sup>35</sup> and AutoAux<sup>36</sup> approaches and the full and reduced algorithms of this work. The universal RI-J and RI-JK auxiliary sets and the MP2 auxiliary set were fully uncontracted for an unbiased comparison with the automatically generated basis sets.

The RI-J sets are aimed at reproducing the Coulomb potential, which tends to be spherically symmetric; thus already low-angular-momentum integrals like (SP|SP) have significant errors. Likewise, the AutoAbs sets target Coulomb integrals. Even though some of the low-angular-momentum integrals are reproduced more accurately by AutoAbs than by the universal RI-J auxiliary sets, the AutoAbs method still exhibits significant errors overall, only halving the total error observed for the universal RI-J auxiliary set.

The RI-JK sets, in turn, have to be able to describe individual orbital densities; this is reflected in smaller errors in small-angular-momentum integrals that describe interactions of

atom	primitive orbital basis	AutoAux basis	full auxiliary basis	reduced auxiliary basis
H	15s5p4d3f1g	17s8p7d6f5g5h	22s19p19d18f15g11h8i4j1k	20s17p15d15f12g10h8i4j1k
He	16s5p4d3f1g	16s8p7d6f6g5h	24s22p22d23f18g11h9i4j1k	23s17p17d14f13g11h9i4j1k
Li	18s12p5d4f3g1h	16s14p13d7f6g5h4i	30s29p25d25f25g23h14i9j7k4l1m	28s24p20d16f14g12h10i9j7k4l1m
Be	19s12p5d4f3g1h	16s13p12d7f6g6h3i	32s29p26d25f26g24h13i10j8k4l1m	29s25p20d17f15g13h11i10j7k4l1m
B	19s13p5d4f3g1h	16s14p13d7f7g6h4i	32s31p27d28f27g26h14i10j8k4l1m	30s26p22d19f17g14h11i10j8k4l1m
C	20s14p5d4f3g1h	16s13p13d7f7g6h4i	31s32p28d28f29g27h15i10j8k4l1m	31s28p23d18f16g14h11i10j8k4l1m
N	20s16p5d4f3g1h	17s15p14d7f7g6h4i	32s32p29d29f30g28h17i11j8k4l1m	32s29p26d21f17g16h13i11j8k4l1m
O	20s15p5d4f3g1h	16s14p13d7f7g6h4i	32s31p29d29f30g28h17i11j8k4l1m	32s28p25d21f17g16h14i11j8k4l1m
F	20s16p5d4f3g1h	16s14p13d7f7g6h4i	33s32p30d29f30g28h17i11j8k4l1m	32s31p26d22f18g16h14i11j8k4l1m
Ne	20s17p5d4f3g1h	17s14p14d7f7g6h4i	32s32p31d30f29g30h17i11j8k4l1m	31s30p28d22f18g16h14i11j8k4l1m
Na	23s18p6d4f3g1h	21s18p17d10f10g9h5i	36s38p36d35f36g35h20i10j7k4l1m	37s35p30d21f16g14h12i10j6k4l1m
Mg	23s18p6d4f3g1h	20s18p17d10f9g9h4i	35s37p35d35f35g35h20i10j7k4l1m	36s35p30d20f14g13h12i10j7k4l1m
Al	23s19p6d4f3g1h	20s17p16d10f9g9h4i	35s38p36d37f36g35h19i10j8k4l1m	35s35p31d20f16g13h11i10j8k4l1m
Si	23s19p6d4f3g1h	20s17p16d10f9g9h5i	35s38p36d36f36g34h20i11j8k4l1m	35s35p30d21f15g14h13i11j8k4l1m
P	23s19p6d4f3g1h	19s17p16d10f9g8h5i	35s36p36d36f35g35h20i11j7k4l1m	34s35p31d22f16g14h13i11j7k4l1m
S	23s19p6d4f3g1h	19s16p16d10f9g8h5i	34s37p36d36f36g35h21i11j8k4l1m	35s36p30d21f16g14h13i11j8k4l1m
Cl	23s19p6d4f3g1h	19s16p15d9f9g8h5i	34s37p35d36f36g35h21i11j8k4l1m	35s34p30d21f16g15h13i11j8k4l1m
Ar	23s19p6d4f3g1h	20s17p16d9f9g8h5i	35s37p36d36f35g34h21i11j8k4l1m	34s35p30d21f16g14h13i11j8k4l1m

Table 2: Composition of 5ZaPa-NR and the resulting AutoAux basis as well as the full and reduced auxiliary basis sets with threshold  $\tau = 10^{-7}$ .



the occupied shells in the iron atom. The RI-JK set still has large errors for high-angular-momentum integrals.

Another interesting point of comparison is offered by the auxiliary basis set for MP2 calculations with the def2-QZVPP orbital basis set (def2-QZVPP-RIFIT). As def2-QZVPP is def2-QZVP with additional polarization functions, the auxiliary basis is sensible also for the studied def2-QZVP orbital basis set. Interesting differences between the accuracy of the MP2 auxiliary basis set and the RI-JK sets can be observed. The MP2 auxiliary basis is noticeably less accurate than the RI-JK set for (SS|SS) and (PD|PD) integrals, which describe interactions between occupied orbitals in the iron atom. But, the MP2 auxiliary basis is noticeably more accurate than the RI-JK set for (DF|DF), (FF|FF), (SG|SG), (PG|PG), and (DG|DG) integrals that arise from polarization as well as electron correlation. The accuracies of the two auxiliary basis sets for other classes of integrals are more or less similar. The total error for the def2-QZVPP-RIFIT auxiliary basis is slightly smaller than for the universal RI-JK set.

Moving onto the general-use basis sets generated by automatic approaches, the AutoAux sets are tailored for computational efficiency at various levels of theory, minimizing the number of auxiliary functions without sacrificing the resulting accuracy; AutoAux especially truncates high-angular-momentum basis functions which are typically not necessary for global fitting approaches. Its total error is smaller than that of the def2-QZVPP-RIFIT auxiliary basis, scoring in at half the error of the universal RI-JK set, and the remaining error is dominated by deficiencies at large angular momentum.

In contrast, the automatically generated auxiliary basis sets from the present approach are able to describe all basis function products that arise from the specified orbital basis, as demonstrated by the small errors in the integrals. Even the (GG|GG) integrals that describe the interactions of the second shell of polarization functions, which are not expected to be important in HF or MP2 calculations, are captured accurately by the present scheme, demonstrating its reliability for any property and any level of theory.

Because the full and reduced schemes appear to afford similar levels of accuracy despite the smaller number of functions involved in the reduced scheme, we will only consider reduced auxiliary basis sets in the remainder of this work unless explicitly specified otherwise.

## 5.2 Accuracy on the W4-17 database

Violin plots<sup>61</sup> whose width demonstrates the distribution of the RI errors in the total energy at the RI-HF and RI-MP2 levels of theory are shown in figures 1 and 2, respectively. The largest RI-HF and RI-MP2 errors encountered in the database are shown in tables 4 and 5 for the AutoAux method of Stoychev et al.<sup>36</sup> and the reduced auxiliary basis method of this work with  $\tau = 10^{-7}$ , respectively.

The errors in the range of millihartrees for the double- $\zeta$  2ZaPa-NR basis set are unacceptably large. The reason for such large errors is that this orbital basis does not include sufficiently many high-angular-momentum functions, which are necessary in the auxiliary basis set in order to describe products of orbital basis functions located on different atoms. This behavior is well-known also in the case of other automated approaches for auxiliary basis set generation. If an auxiliary basis set is needed for a small orbital basis set, an auxiliary basis generated for a larger orbital basis set should be used instead to guarantee sufficiently small RI errors.

The RI errors in the total energies in both RI-HF and RI-MP2 calculations for triple- $\zeta$  and larger basis sets are small, ranging only up to tens of microhartree as shown by table 5, while the AutoAux method yields somewhat larger errors in total energies as shown by table 4. However, even the largest error of  $1.53 \times 10^{-4} E_h$  in the RI-MP2/5ZaPa-NR total energies with the AutoAux method is less than 0.1 kcal/mol. Moreover, as errors in total energies tend to cancel out in applications, both AutoAux and the present algorithm with a suitably small value for  $\tau$  appear to be reliable ways to generate auxiliary basis sets for applications.

integral type	def2-universal-jfit 19s14p12d10f7g3h1i	def2-universal-jkfit 19s13p11d8f7g5h2i	def2-QZVPP-RIFIT 15s13p11d8f7g5h2i	AutoAbs 24s19p14d8f7g	AutoAux 22s19p18d17f16g6h4i	full $\tau = 10^{-7}$ 36s38p39d38f37g24h12i4j1k	reduced $\tau = 10^{-7}$ 38s36p33d28f25g15h10i4j1k
(SS SS)	$6.878 \times 10^{-5}$	$1.283 \times 10^{-4}$	$1.942 \times 10^{-3}$	$7.274 \times 10^{-5}$	$9.411 \times 10^{-6}$	$1.217 \times 10^{-5}$	$9.466 \times 10^{-6}$
(SP SP)	$2.661 \times 10^0$	$2.864 \times 10^{-4}$	$2.833 \times 10^{-4}$	$2.400 \times 10^{-4}$	$3.692 \times 10^{-6}$	$1.233 \times 10^{-6}$	$6.744 \times 10^{-7}$
(PP PP)	$1.086 \times 10^0$	$8.635 \times 10^{-3}$	$1.098 \times 10^{-2}$	$2.707 \times 10^{-3}$	$1.075 \times 10^{-4}$	$5.518 \times 10^{-6}$	$9.908 \times 10^{-7}$
(SD SD)	$8.620 \times 10^{-2}$	$2.051 \times 10^{-4}$	$4.392 \times 10^{-4}$	$7.592 \times 10^{-4}$	$9.842 \times 10^{-6}$	$2.279 \times 10^{-7}$	$1.294 \times 10^{-7}$
(PD PD)	$5.723 \times 10^{-1}$	$1.221 \times 10^{-3}$	$4.604 \times 10^{-2}$	$6.614 \times 10^{-2}$	$1.207 \times 10^{-4}$	$2.826 \times 10^{-6}$	$1.438 \times 10^{-6}$
(DD DD)	$5.656 \times 10^{-1}$	$1.394 \times 10^{-1}$	$9.993 \times 10^{-2}$	$8.098 \times 10^{-2}$	$2.926 \times 10^{-4}$	$7.261 \times 10^{-5}$	$2.361 \times 10^{-5}$
(SF SF)	$5.295 \times 10^{-1}$	$1.265 \times 10^{-3}$	$9.474 \times 10^{-4}$	$1.105 \times 10^{-2}$	$4.507 \times 10^{-5}$	$5.630 \times 10^{-7}$	$2.322 \times 10^{-6}$
(PF PF)	$1.437 \times 10^{-1}$	$1.702 \times 10^{-3}$	$1.002 \times 10^{-3}$	$7.409 \times 10^{-2}$	$1.149 \times 10^{-4}$	$1.216 \times 10^{-6}$	$1.413 \times 10^{-6}$
(DF DF)	$2.490 \times 10^0$	$6.310 \times 10^{-2}$	$1.113 \times 10^{-2}$	$2.046 \times 10^0$	$1.059 \times 10^{-2}$	$4.809 \times 10^{-5}$	$4.257 \times 10^{-5}$
(FF FF)	$2.191 \times 10^0$	$9.606 \times 10^{-1}$	$3.803 \times 10^{-1}$	$2.018 \times 10^0$	$3.901 \times 10^{-2}$	$3.391 \times 10^{-4}$	$3.498 \times 10^{-4}$
(SG SG)	$1.986 \times 10^{-2}$	$6.502 \times 10^{-4}$	$1.344 \times 10^{-4}$	$9.036 \times 10^{-4}$	$3.083 \times 10^{-5}$	$3.469 \times 10^{-8}$	$8.586 \times 10^{-8}$
(PG PG)	$7.234 \times 10^{-1}$	$1.180 \times 10^{-2}$	$1.146 \times 10^{-3}$	$5.159 \times 10^{-1}$	$1.807 \times 10^{-3}$	$1.354 \times 10^{-6}$	$4.869 \times 10^{-7}$
(DG DG)	$7.276 \times 10^{-1}$	$1.948 \times 10^{-1}$	$5.872 \times 10^{-2}$	$6.714 \times 10^{-1}$	$1.391 \times 10^{-2}$	$4.954 \times 10^{-6}$	$3.183 \times 10^{-6}$
(FG FG)	$1.604 \times 10^0$	$6.855 \times 10^{-1}$	$6.610 \times 10^{-1}$	$1.267 \times 10^0$	$6.576 \times 10^{-1}$	$4.911 \times 10^{-5}$	$7.325 \times 10^{-5}$
(GG GG)	$8.942 \times 10^{-1}$	$5.624 \times 10^{-1}$	$5.218 \times 10^{-1}$	$8.378 \times 10^{-1}$	$4.581 \times 10^{-1}$	$2.033 \times 10^{-4}$	$1.493 \times 10^{-4}$
total	$2.385 \times 10^1$	$3.592 \times 10^0$	$2.577 \times 10^0$	$1.225 \times 10^1$	$1.866 \times 10^0$	$8.519 \times 10^{-4}$	$7.843 \times 10^{-4}$

Table 3: Error  $\Delta$  in the diagonal repulsion integrals  $(\mu\nu|\mu\nu)$  in Hartree for the Fe atom in the def2-QZVP basis set employing the fully uncontracted universal jfit<sup>19</sup> and jkfit<sup>20</sup> basis sets, the auxiliary basis for MP2 calculations of the def2-QZVPP orbital basis set (def2-QZVPP-RIFIT),<sup>23</sup> as well as automatically generated sets using the AutoAbs<sup>35</sup> and AutoAux<sup>36</sup> methods as well as the full and reduced schemes of this work.

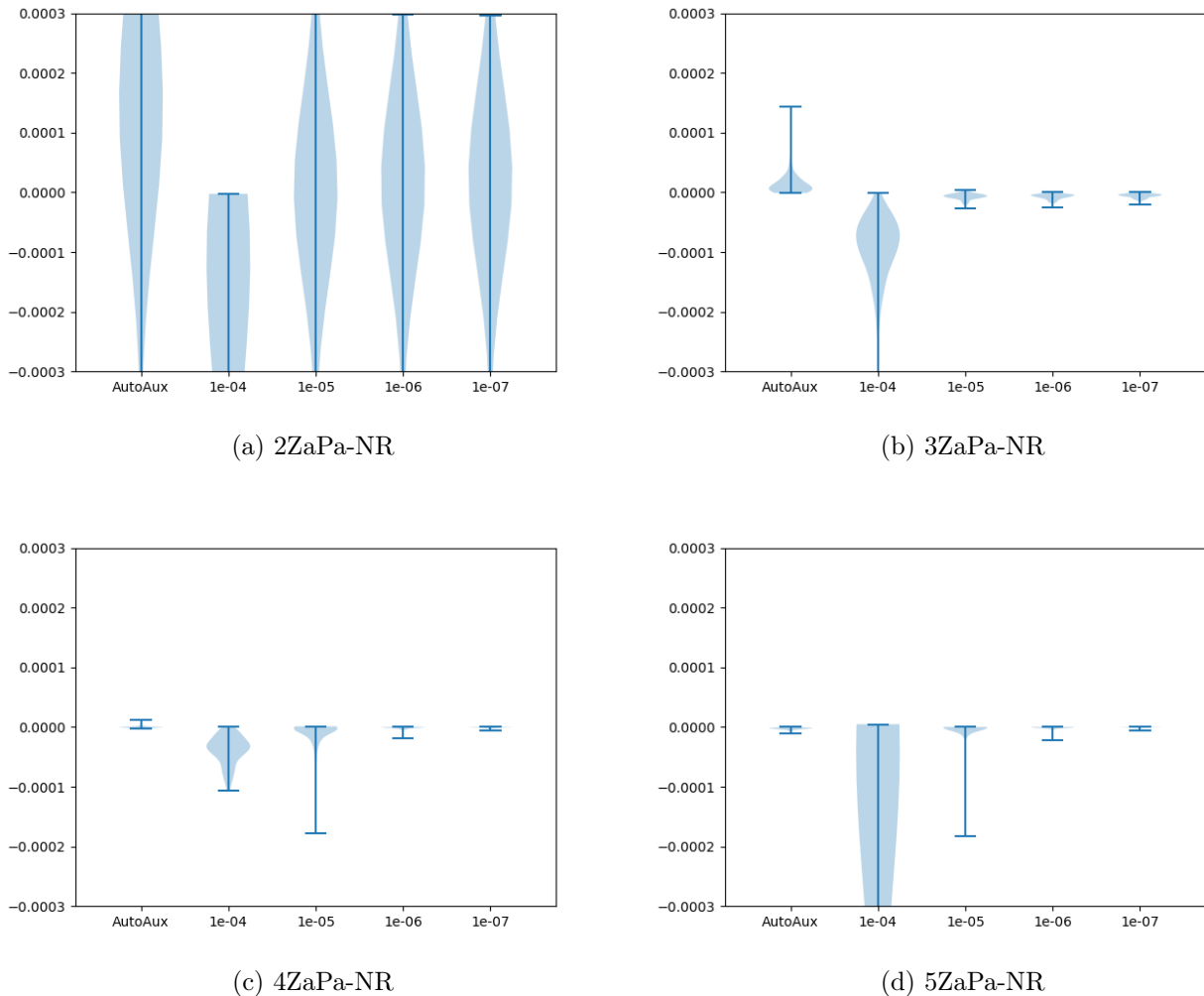


Figure 1: RI errors in  $E_h$  in the RI-HF total energy of the W4-17 dataset for the AutoAux method and the reduced auxiliary basis obtained with  $\tau = 10^{-4}$ ,  $\tau = 10^{-5}$ ,  $\tau = 10^{-6}$ , and  $\tau = 10^{-7}$ .

Table 4: Largest RI errors in the database employing the AutoAux method.<sup>36</sup>

orbital basis	RI-HF ( $E_h$ )	molecule	RI-MP2 ( $E_h$ )	molecule
2ZaPa-NR	$5.67 \times 10^{-3}$	c-hooo	$9.07 \times 10^{-3}$	c-hooo
3ZaPa-NR	$1.44 \times 10^{-4}$	hclo4	$1.12 \times 10^{-4}$	c2cl6
4ZaPa-NR	$1.18 \times 10^{-5}$	hclo4	$1.06 \times 10^{-4}$	c2cl6
5ZaPa-NR	$1.11 \times 10^{-5}$	p4	$1.53 \times 10^{-4}$	c2cl6

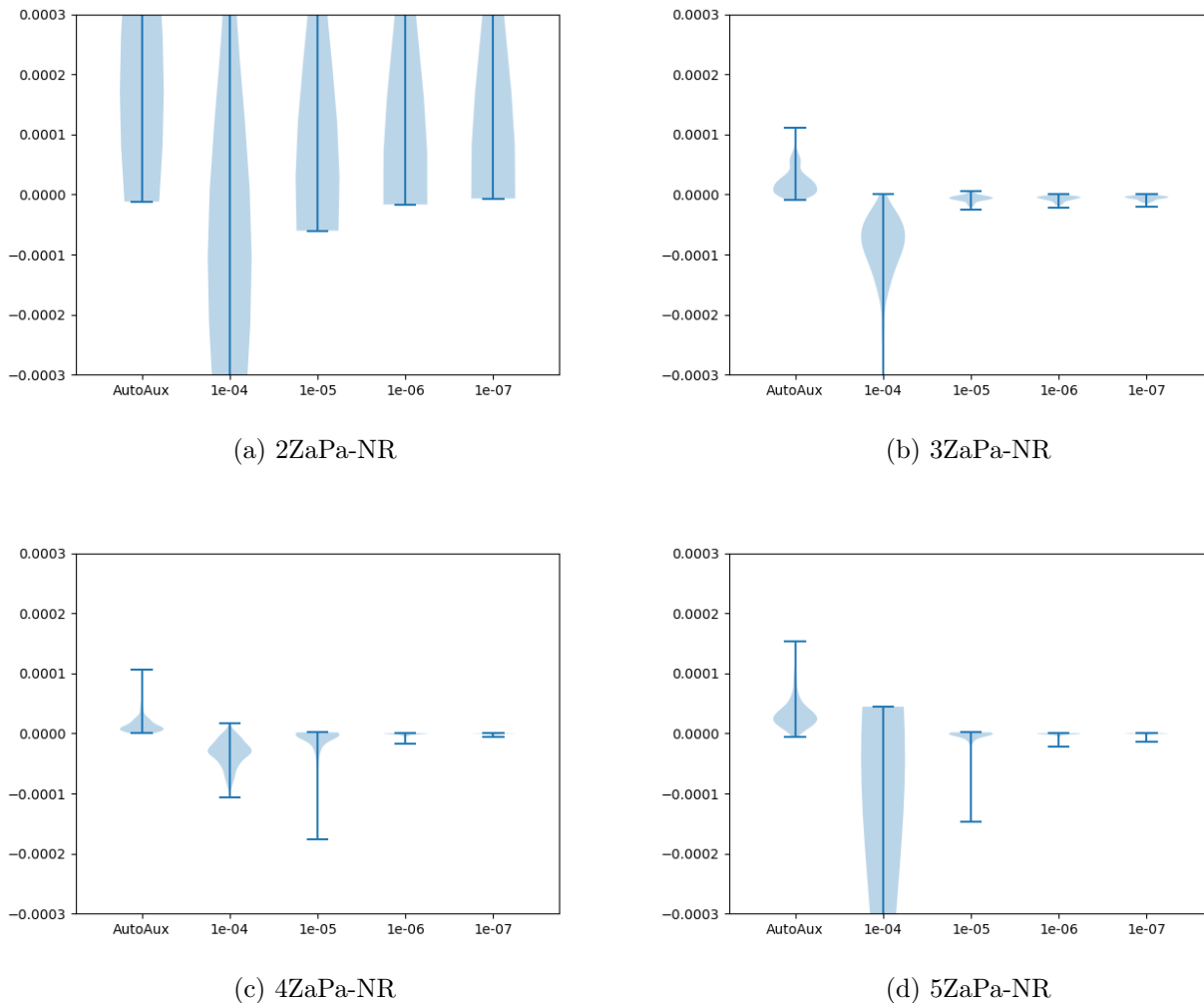


Figure 2: RI errors in  $E_h$  in the RI-MP2 total energy of the W4-17 dataset for the AutoAux method and the reduced auxiliary basis obtained with  $\tau = 10^{-4}$ ,  $\tau = 10^{-5}$ ,  $\tau = 10^{-6}$ , and  $\tau = 10^{-7}$ .

Table 5: Largest RI errors in the database employing the reduced auxiliary basis method of this work with  $\tau = 10^{-7}$ .

orbital basis	RI-HF ( $E_h$ )	molecule	RI-MP2 ( $E_h$ )	molecule
2ZaPa-NR	$5.97 \times 10^{-3}$	c-hooo	$8.82 \times 10^{-3}$	c-hooo
3ZaPa-NR	$2.00 \times 10^{-5}$	c2cl6	$1.97 \times 10^{-5}$	c2cl6
4ZaPa-NR	$5.37 \times 10^{-6}$	dithiotane	$5.25 \times 10^{-6}$	dithiotane
5ZaPa-NR	$6.65 \times 10^{-6}$	c2cl6	$1.40 \times 10^{-5}$	benzene

### 5.3 Timing benchmark

To further illustrate the usefulness of the RI approach and automatically generated auxiliary basis sets, we consider calculations on commodity hardware with free and open source software whose advantages for computational chemistry has recently been discussed in ref. 62. As a practical example, we consider HF and MP2 calculations on small water clusters with tight-binding geometries from ref. 63. The 3ZaPa-NR orbital basis set<sup>58</sup> is used, and the calculations are carried out with the PSI4 program<sup>13</sup> with various auxiliary basis sets: in addition to sets generated using the algorithm of this work with various values for  $\tau$ , we also consider the AutoAux algorithm. Because the present algorithm employs uncontracted basis sets, data are also included for an AutoAux basis generated for the 3ZaPa-NR basis in fully uncontracted form (denoted as AutoAux\*).

Before reporting the employed methodology and the resulting timings, it is imperative to discuss the general limitations of published benchmarks timings, which are well-known to be a sensitive topic in quantum chemistry: in fact, some programs go as far as to forbid reporting performance data altogether because of the issues discussed below.

Obviously, the timings depend on the employed hardware. The present calculations are performed on a commodity cloud server with an Intel Xeon W3520 processor running at 2.67GHz, with 16 GB of memory. The timings also depend the compiler as well as the employed compiler options, linear algebra and two-electron integral libraries, and so on. For simplicity, we employ the Fedora package of PSI4 version 1.3.2 on Fedora 34 (`psi4-1.3.2-10.fc34.x86_64`), and have not attempted to tune its performance in any way. (Note that the RI calculations reported in section 5.2 were also performed on the same hardware and program package.)

An even bigger impact on timings arise from the used program. The employed algorithm has a huge impact: for instance, the evaluation of the MP2 correlation energy by direct methods<sup>64</sup> becomes highly appealing for large systems, but such an algorithm is not available in PSI4 at present. Different programs may also employ different numerical thresholds by

default, meaning they are actually performing different types of calculations. All of these issues should be kept in mind when examining the timing data presented below, whose only purpose is to illustrate considerations in running practical computations with PSI4.

Disk-based algorithms (`scf_type pk` and `mp2_type conv`) were used for the conventional calculations, whereas the RI calculations employed `scf_type df` and `mp2_type df`; also other types of SCF and MP2 algorithms are available in PSI4, but they were not considered for the present benchmark. The calculations employ 4 threads, 14 GB of memory, and the default convergence and accuracy thresholds in PSI4. The resulting wall times are shown in table 6, while the binding energies and RI errors therein are shown in table 7.

As can be seen from table 6, while the conventional algorithm is slightly faster for the smallest systems, there is a crossover whose position depends on the employed auxiliary basis, after which the RI calculations become significantly faster than the conventional algorithm. While the conventional MP2 calculation for the two-molecule cluster still employs an in-core algorithm, the MP2 step of the three-molecule cluster employs a partly out-of-core algorithm, resulting in the considerable wall time difference between the HF and MP2 calculations for this system. An even larger jump in the computational cost of the conventional algorithm is observed for both HF and MP2 calculations on the four-molecule cluster, for which the two-electron integrals no longer fit in memory. At variance, the RI integrals fit in memory even for the largest computations considered, and no sudden jumps in the computational cost are observed for the RI calculations.

The AutoAux algorithm, which has a large number of parameters that have been optimized to yield the smallest possible auxiliary basis sets that still are accurate enough for routine applications, is competitive with the conventional algorithm even for the smallest system size studied, the water molecule. The AutoAux algorithm replaces contracted Gaussian functions with an effective Gaussian primitive. Comparison of the timings for the AutoAux auxiliary basis sets generated for the 3ZaPa-NR basis in its original contracted and fully uncontracted form shows that this design aspect of the AutoAux algorithm has a significant

effect on its computational performance: the calculations that employ an auxiliary basis generated for the 3ZaPa-NR basis in uncontracted form are 2–3 times slower.

Interestingly, as can be seen by studying the data in figures 1 and 2 and tables 6 and 7, the accuracy and computational performance of the present algorithm with  $\tau = 10^{-5}$  appears to be roughly comparable to AutoAux for uncontracted basis sets, even though AutoAux is a heavily optimized semiempirical algorithm with tens of parameters that also truncates the high-angular-momentum functions, while the present algorithm is controlled by a single parameter, allowing an easy adjustment of the computational cost / accuracy ratio, and no further truncation of high-angular-momentum functions has been attempted in this work. Moreover, the present algorithm affords more accurate results (with respect to the complete auxiliary basis set limit) at only slightly increased computational cost by the use of a smaller value of  $\tau$ , such as  $\tau = 10^{-6}$ . These results are highly promising for future applications of the present algorithm to Slater-type orbital and numerical atomic orbital basis sets: the auxiliary basis sets generated by the present algorithm are competitive with ones from the heavily optimized AutoAux algorithm when uncontracted basis sets are employed, proving the expected optimal nature of the present algorithm.

## 5.4 Importance of reordering: case study

As a final point, we will investigate the importance of the reordering of the auxiliary function candidates before the pivoted Cholesky decomposition. As the ordering presumably becomes more important for larger basis sets, we will examine the 5ZaPa-NR orbital basis for this part of the study, and employ the full algorithm to maximize the number of candidates.

We begin by examining the P shell of auxiliary functions for Ar, for which the full algorithm leads to 818 primitive candidate functions. Performing 10 000 random permutations of the 818 primitives and running the pivoted Cholesky algorithm on each of them, we obtain the distribution shown in figure 3. In contrast, feeding in the candidates in numerical order of the exponents, or ordering the candidate functions in increasing off-diagonal overlap both



Table 6: Total wall times in seconds for HF and MP2 calculations on water clusters in the 3ZaPa-NR orbital basis, using either an RI algorithm with automatically generated basis sets with the present algorithm with various values for  $\tau$  or the AutoAux method,<sup>36</sup> or the conventional algorithm (conv). AutoAux\* denotes an AutoAux basis generated for an uncontracted orbital basis. The timings for the MP2 calculations also include the HF step.

(a) HF								
	$\tau = 10^{-3}$	$\tau = 10^{-4}$	$\tau = 10^{-5}$	$\tau = 10^{-6}$	$\tau = 10^{-7}$	AutoAux*	AutoAux	conv
H <sub>2</sub> O	3.9	4.1	4.2	4.4	4.5	4.2	3.8	3.8
(H <sub>2</sub> O) <sub>2</sub>	6.4	8.0	9.6	10.8	12.0	9.2	5.9	9.7
(H <sub>2</sub> O) <sub>3</sub>	13.9	20.1	26.0	31.4	36.5	25.9	12.4	34.9
(H <sub>2</sub> O) <sub>4</sub>	29.1	44.0	59.7	72.1	103.5	56.4	25.2	1492.5
(H <sub>2</sub> O) <sub>5</sub>	80.5	127.1	160.6	184.1	212.6	151.2	51.3	3951.3

(b) MP2								
	$\tau = 10^{-3}$	$\tau = 10^{-4}$	$\tau = 10^{-5}$	$\tau = 10^{-6}$	$\tau = 10^{-7}$	AutoAux*	AutoAux	conv
H <sub>2</sub> O	5.0	5.4	8.9	5.9	6.2	5.5	4.7	4.6
(H <sub>2</sub> O) <sub>2</sub>	8.8	11.6	14.0	16.3	18.4	13.6	8.1	27.8
(H <sub>2</sub> O) <sub>3</sub>	20.4	30.2	40.4	48.9	57.6	39.7	18.0	221.7
(H <sub>2</sub> O) <sub>4</sub>	43.3	67.2	93.1	112.8	152.1	86.0	36.8	2408.5
(H <sub>2</sub> O) <sub>5</sub>	115.3	178.6	233.4	268.0	314.0	212.3	76.7	7424.0

Table 7: HF and MP2 binding energies  $E_{\text{bind}}(n) = nE[\text{H}_2\text{O}] - E[(\text{H}_2\text{O})_n]$  of water clusters in eV, as well as the corresponding RI errors  $\Delta E_{\text{bind}}(n) = E_{\text{bind}}^{\text{conventional}}(n) - E_{\text{bind}}^{\text{RI}}(n)$  for various automatically generated auxiliary basis sets in meV. All calculations employ the 3ZaPa-NR orbital basis set and tight-binding geometries from ref. 63. The notation is otherwise analogous to that in table 6.

(a) HF								
	$E_{\text{bind}}^{\text{conventional}}$	$\tau = 10^{-3}$	$\tau = 10^{-4}$	$\tau = 10^{-5}$	$\tau = 10^{-6}$	$\tau = 10^{-7}$	AutoAux*	AutoAux
(H <sub>2</sub> O) <sub>2</sub>	0.130	0.051	0.065	-0.000	0.004	0.003	-0.001	-0.001
(H <sub>2</sub> O) <sub>3</sub>	0.372	0.084	0.094	-0.004	0.032	0.021	-0.010	-0.001
(H <sub>2</sub> O) <sub>4</sub>	0.703	0.107	0.131	-0.004	0.041	0.028	-0.007	0.004
(H <sub>2</sub> O) <sub>5</sub>	0.971	0.153	0.164	-0.005	0.046	0.042	-0.009	0.006

(b) MP2								
	$E_{\text{bind}}^{\text{conventional}}$	$\tau = 10^{-3}$	$\tau = 10^{-4}$	$\tau = 10^{-5}$	$\tau = 10^{-6}$	$\tau = 10^{-7}$	AutoAux*	AutoAux
(H <sub>2</sub> O) <sub>2</sub>	0.216	0.097	0.073	0.000	0.004	0.003	-0.011	-0.009
(H <sub>2</sub> O) <sub>3</sub>	0.662	0.190	0.110	-0.004	0.031	0.020	-0.042	-0.028
(H <sub>2</sub> O) <sub>4</sub>	1.204	0.267	0.158	-0.003	0.039	0.025	-0.076	-0.058
(H <sub>2</sub> O) <sub>5</sub>	1.580	0.353	0.200	-0.003	0.044	0.039	-0.105	-0.083

result in 37 primitives—which coincides with the maximum of the distribution in figure 3. Thus, even though some of the randomized initial orderings resulted in a slightly smaller number of auxiliary functions, the level of performance for the presently employed algorithm is satisfactory.

Moving on to the comparison of the compositions of the complete auxiliary basis sets for the 5ZaPa-NR orbital basis resulting from ordering the candidates on the individual shells of the individual elements H–Ar either by i) numerical value or ii) off-diagonal Coulomb overlap, only small differences are observed (not shown): most shells end up with the same number of functions, while the others differ only by the addition or removal of a single function. Although mixed performance is observed for methods i) and ii), with method i) sometimes yielding fewer functions than method ii), method ii) yields the fewest number of functions overall. Future implementations of the present algorithm may attempt to minimize the size of the generated auxiliary basis by trying out several initial orderings of the candidate functions before the pivoted Cholesky decomposition, and picking the one that leads to the most compact decomposition i.e. smallest auxiliary basis set for each shell.

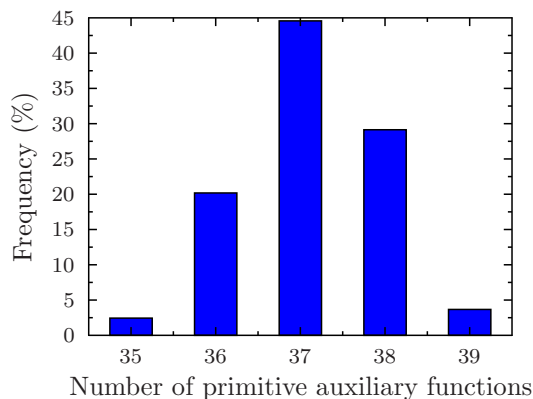


Figure 3: Distribution of the number of P primitives in automatically generated auxiliary basis sets for the 5ZaPa-NR orbital basis for Ar, sampled for 10 000 random permutations of the 818 candidate functions.

## 6 Summary and discussion

We have presented a general method to form auxiliary basis sets in linear combination of atomic orbitals calculations. In addition to commonly-used Gaussian basis sets, the method is also straightforwardly applicable to use with Slater-type orbitals and numerical atomic orbitals, and we hope to pursue such applications in future work. The algorithm can be implemented in a simple-minded manner from the full set of orbital products; alternatively, a Cholesky decomposition of the atomic two-electron integrals tensor can be used to screen the set of candidate functions, leading to auxiliary basis sets with considerably fewer functions at intermediate angular momenta.

We have benchmarked the accuracy of the reduced auxiliary basis sets in proof-of-concept applications to Hartree–Fock and second-order Møller–Plesset perturbation theory calculations on the non-multireference part of the W4-17 database of molecules, and shown that the resulting fitting errors in total energies are negligible for basis sets of at least polarized triple- $\zeta$  quality. The Gaussian auxiliary basis sets obtained with the present algorithm compare favorably in accuracy and computational cost to the heavily parametrized AutoAux method<sup>36</sup> when the orbital basis is not contracted. These results are promising for the future applications with Slater-type and numerical atomic orbital basis sets, for which the computation of the exact two-electron integrals is difficult.

As the full auxiliary sets are larger than the reduced auxiliary basis sets, they are expected to be at least as accurate as the reduced auxiliary basis sets. Therefore they should likewise be useful in applications where Cholesky decompositions of the atomic two-electron integrals tensor are not available. The full auxiliary basis set algorithm, which was presented in algorithm 1, is similar to the one of Ren et al.<sup>17</sup>; the main difference being that their Gram–Schmidt procedure is replaced by the pivoted Cholesky decomposition. Thus, implementing the present method in existing implementations of the Ren et al. algorithm should be extremely straightforward. (As a further difference, we also suggest reordering the auxiliary function candidates in increasing off-diagonal overlap.)

The automated schemes pursued in this work as well as refs. 17 and 41 do not truncate high-angular-momentum functions unlike e.g. the schemes of Yang et al.<sup>35</sup> and Stoychev et al.<sup>36</sup> Although the high-angular-momentum functions can usually be discarded for global Coulomb and exchange fitting, the situation is different for e.g. local fitting algorithms that may be used to circumvent the steep computational scaling of global fitting methods.<sup>39</sup> Possible strategies for further truncation of the generated auxiliary basis sets may be investigated in future work.

Because the procedure of this work is able to generate auxiliary basis sets of varying precision, and because the auxiliary basis set arising from the decomposition of equation (7) to threshold  $\tau_1$  is a subset of the one obtained for  $\tau_2 < \tau_1$ , the present algorithm could be easily paired with e.g. dual auxiliary basis set approaches,<sup>65</sup> in analogy to the established practice of employing Cholesky decompositions of the two-electron integrals of varying thresholds<sup>66</sup> to speed up self-consistent field calculations.

As was already discussed in refs. 46 and 47, the pivoted Cholesky procedure depends somewhat on the initial ordering of the basis functions, as the (Coulomb) overlap matrix has a unit diagonal. This work used the self-sufficient method introduced in ref. 47 of ordering the functions in increasing off-diagonal overlap. But, it was also found that slightly more compact decompositions, that is, auxiliary basis sets can be found in some cases by a randomized search. As generating the auxiliary basis is inexpensive compared to the subsequent electronic structure calculations, future implementations of the present algorithm may consider employing quasi-exhaustive searches to minimize the size of the generated auxiliary basis set, even though only small differences are expected in the resulting numbers of primitive functions.

In this work, we have employed the pivoted Cholesky procedure of refs. 46 and 47 to choose the auxiliary functions from a pool of candidate functions. As our last point, we wish to note that the same algorithm can also be used to choose linearly independent sets of auxiliary functions in *molecular calculations*. Overcompleteness issues with the auxiliary basis

set are expected in molecular calculations with extended basis sets such as those developed in ref. 34; the modeling of weakly bound electrons<sup>67</sup> also often involves extremely diffuse basis functions.<sup>46</sup> The density-fitted two-electron integrals of equation (1) can be written as  $(\mu\nu|\sigma\rho) = \sum_A B_{\mu\nu}^A B_{\sigma\rho}^A$ , where the ‘‘B matrix’’ is defined as  $B_{\mu\nu}^A = \sum_B (A|B)^{-1/2} (B|\mu\nu)$ . The formation of  $(A|B)^{-1/2}$  is analogous to the canonical orthogonalization algorithm for orbital basis sets,<sup>68</sup> and may be numerically ill-conditioned. However, continuing the analogy,  $(A|B)^{-1/2}$  can be formed in a numerically stable manner by employing the procedure of refs. 46 and 47: a pivoted Cholesky decomposition on  $S_{AB} = (A|B)$  can be used to pick a linearly independent subset of auxiliary functions for the molecule, which can then be employed to carry out the calculation.

## Appendix I. Coulomb overlap integrals

As is well known,<sup>14,50</sup> one-center two-electron integrals reduce to a product of radial and angular integrals through the Laplace expansion

$$\frac{1}{r_{12}} = \frac{4\pi}{r_{>}} \sum_{L=0}^{\infty} \frac{1}{2L+1} \left(\frac{r_{<}}{r_{>}}\right)^L \sum_{M=-L}^L Y_L^M(\Omega_1) (Y_L^M(\Omega_2))^*.$$

The case of four-index integrals leads to the need to evaluate Gaunt coefficients and various types of integrals; see ref. 50 for discussion. However, as the present scheme only requires two-index integrals, only simple radial integrals are necessary due to the orthonormality of the spherical harmonics

$$(A|B) = \int \frac{\chi_A^*(\mathbf{r})\chi_B(\mathbf{r}')}{|\mathbf{r} - \mathbf{r}'|} d^3r d^3r' = \frac{\delta_{l_A l_B}}{2l_A + 1} \int_0^\infty dr r^2 \int_0^\infty dr' r'^2 \frac{4\pi}{r_{>}} \left(\frac{r_{<}}{r_{>}}\right)^{l_A} \chi_A(r)\chi_B(r') \quad (13)$$

The radial integral can be rewritten in a form more suitable for computation as

$$\begin{aligned}
(A|B) &= \iint \chi_A(r)\chi_B(r') \frac{r^l}{r^{l+1}} r^2 dr r'^2 dr' \\
&= \int_0^\infty dr r^2 \int_0^r dr' r'^2 [f(r)g(r') + f(r')g(r)] \frac{r^l}{r^{l+1}} \\
&= \int_0^\infty dr r^{2-l-1} \int_0^r dr' r'^{2+l} [f(r)g(r') + f(r')g(r)]
\end{aligned}$$

## Gaussian type orbitals

Spherical harmonic Gaussian type orbitals (GTOs) have the form

$$\chi_A^{\text{GTO}}(r) = r^{l_A} e^{-\alpha_A r^2} Y_{l_A}^{m_A}(\hat{\mathbf{r}})$$

which yields

$$\begin{aligned}
(A|B)^{\text{GTO}} &= \int_0^\infty dr r^{2-l-1} \int_0^r dr' r'^{2+l} [f(r)g(r') + f(r')g(r)] \delta_{l_A} \delta_{l_B} \\
&= \int_0^\infty dr r \int_0^r dr' r'^{2+2l} \left[ e^{-\alpha_A r^2 - \alpha_B r'^2} + e^{-\alpha_A r'^2 - \alpha_B r^2} \right] \delta_{l_A} \delta_{l_B} \\
&= \frac{1}{4} \Gamma\left(l + \frac{3}{2}\right) \frac{(\alpha_A + \alpha_B)^{-l-1/2}}{\alpha_A \alpha_B} \delta_{l_A} \delta_{l_B}
\end{aligned}$$

with Mathematica 12.1.

## General Slater type orbitals

Slater type orbitals (STOs) have the general form

$$\chi_A^{\text{STO}}(r) = r^{n_A-1} e^{-\alpha_A r} Y_{l_A}^{m_A}(\hat{\mathbf{r}})$$

which yields

$$\begin{aligned} & \int_0^\infty dr r^{1-l} \int_0^r dr' r'^{2+l} [f(r)g(r') + f(r')g(r)] \\ &= \int_0^\infty dr r^{-l} \int_0^r dr' r'^{l+1} \left[ r^{n_A} r'^{n_B} e^{-\alpha_A r^2 - \alpha_B r'^2} + r^{n_B} r'^{n_A} e^{-\alpha_A r'^2 - \alpha_B r^2} \right] \end{aligned}$$

Evaluation with Mathematica 12.1 leads to

$$\begin{aligned} & \alpha_A^{-2-L-n_A} \alpha_B^{-1+L-n_B} \Gamma(2+L+n_A) \Gamma(1-L+n_B) \\ &+ \alpha_A^{-1+L-n_A} \alpha_B^{-2-L-n_B} \Gamma(1-L+n_A) \Gamma(2+L+n_B) \\ &- \Gamma(3+n_A+n_B) \times \left[ \frac{\alpha_B^{-3-n_A-n_B} {}_2F_1\left(1-L+n_A, 3+n_A+n_B, 2-L+n_A, -\frac{\alpha_A}{\alpha_B}\right)}{1-L+n_A} \right. \\ & \left. \frac{\alpha_A^{-3-n_A-n_B} {}_2F_1\left(1-L+n_B, 3+n_A+n_B, 2-L+n_B, -\frac{\alpha_B}{\alpha_A}\right)}{1-L+n_B} \right] \end{aligned}$$

where  ${}_2F_1$  is the ordinary hypergeometric function.

## Even-tempered Slater type orbitals

Even-tempered STOs pick the lowest possible primary quantum number for all angular momentum channels, i.e.  $n_A = l_A + 1$ , so that the radial functions become analogous to GTOs

$$\chi_A^{\text{ET-STO}}(r) = r^{l_A} e^{-\zeta_A r} Y_{l_A}^{m_A}(\hat{\mathbf{r}})$$

yielding a simpler expression

$$(A|B)^{\text{ET-STO}} = \frac{[\zeta_A^2 + \zeta_B^2 + \zeta_A \zeta_B (3+2l)] \Gamma(3+2l)}{\zeta_A^2 \zeta_B^2 (\zeta_A + \zeta_B)^{3+2l}} \delta_{l_A} \delta_{l_B}$$

## Appendix II. Effective Gaussian exponents

The radial expectation value for a given radial function  $R(r) = r^l e^{-\alpha r^2}$  is

$$\langle r \rangle = \frac{\int_0^\infty r^3 R(r)^2 dr}{\int_0^\infty r^2 R(r)^2 dr} = \frac{\Gamma(l+2)}{\Gamma(l+\frac{3}{2})\sqrt{2\alpha}}. \quad (14)$$

This means that the contribution of a given product function  $r^{l_i+l_j} e^{-(\alpha_i+\alpha_j)r^2}$  into the angular momentum channel  $|l_i - l_j| \leq L \leq l_i + l_j$  is best approximated by the function that satisfies

$$\frac{\Gamma(L+2)}{\Gamma(L+\frac{3}{2})\sqrt{2\alpha_{\text{eff}}}} = \frac{\Gamma(l_i+l_j+2)}{\Gamma(l_i+l_j+\frac{3}{2})\sqrt{2(\alpha_i+\alpha_j)}} \quad (15)$$

from which

$$\alpha_{\text{eff}} = \left[ \frac{\Gamma(L+2)\Gamma(l_i+l_j+\frac{3}{2})}{\Gamma(l_i+l_j+2)\Gamma(L+\frac{3}{2})} \right]^2 (\alpha_i + \alpha_j) \quad (16)$$

The gamma function scaling factor in equation (16) is unity for  $L = l_i + l_j$  and decreases monotonically for  $L < l_i + l_j$  because in that case  $r^{l_i+l_j}$  results in a more diffuse character for the product wave function than  $r^L$  does, which is taken into account by scaling down the exponent; for instance, for a  $g \times g$  product coupling to  $L = 0$  the scale factor is roughly 0.1375.

## Acknowledgments

We thank Frank Neese and Georgi Stoychev for assistance in verifying the Basis Set Exchange implementation of the AutoAux method, Roland Lindh for discussions on the acCD method, as well as Volker Blum for discussions on local fitting methods. We thank the National Science Foundation for financial support under Grant No. CHE-2136142.



## References

- (1) Whitten, J. L. Coulombic potential energy integrals and approximations. *J. Chem. Phys.* **1973**, *58*, 4496.
- (2) Baerends, E. J.; Ellis, D. E.; Ros, P. Self-consistent molecular Hartree–Fock–Slater calculations I. The computational procedure. *Chem. Phys.* **1973**, *2*, 41–51.
- (3) Dunlap, B. I.; Connolly, J. W. D.; Sabin, J. R. On the applicability of LCAO- $X\alpha$  methods to molecules containing transition metal atoms: The nickel atom and nickel hydride. *Int. J. Quantum Chem.* **1977**, *12*, 81–87.
- (4) Dunlap, B. I.; Connolly, J. W. D.; Sabin, J. R. On some approximations in applications of  $X\alpha$  theory. *J. Chem. Phys.* **1979**, *71*, 3396.
- (5) Dunlap, B. I.; Rösch, N.; Trickey, S. B. Variational fitting methods for electronic structure calculations. *Mol. Phys.* **2010**, *108*, 3167–3180.
- (6) Vahtras, O.; Almlöf, J.; Feyereisen, M. W. Integral approximations for LCAO-SCF calculations. *Chem. Phys. Lett.* **1993**, *213*, 514–518.
- (7) Eichkorn, K.; Treutler, O.; Ohm, H.; Haser, M.; Ahlrichs, R. Auxiliary basis sets to approximate Coulomb potentials. *Chem. Phys. Lett.* **1995**, *240*, 283–289.
- (8) Weigend, F. A fully direct RI-HF algorithm: Implementation, optimised auxiliary basis sets, demonstration of accuracy and efficiency. *Phys. Chem. Chem. Phys.* **2002**, *4*, 4285–4291.
- (9) Manzer, S.; Horn, P. R.; Mardirossian, N.; Head-Gordon, M. Fast, accurate evaluation of exact exchange: The occ-RI-K algorithm. *J. Chem. Phys.* **2015**, *143*, 024113.
- (10) Feyereisen, M.; Fitzgerald, G.; Komornicki, A. Use of approximate integrals in ab initio theory. An application in MP2 energy calculations. *Chem. Phys. Lett.* **1993**, *208*, 359–363.

- (11) Weigend, F.; Häser, M.; Patzelt, H.; Ahlrichs, R. RI-MP2: optimized auxiliary basis sets and demonstration of efficiency. *Chem. Phys. Lett.* **1998**, *294*, 143–152.
- (12) Shiozaki, T. BAGEL: Brilliantly Advanced General Electronic-structure Library. *Wiley Interdiscip. Rev. Comput. Mol. Sci.* **2018**, *8*, e1331.
- (13) Smith, D. G. A.; Burns, L. A.; Simmonett, A. C.; Parrish, R. M.; Schieber, M. C.; Galvelis, R.; Kraus, P.; Kruse, H.; Di Remigio, R.; Alenaizan, A.; James, A. M.; Lehtola, S.; Misiewicz, J. P.; Scheurer, M.; Shaw, R. A.; Schriber, J. B.; Xie, Y.; Glick, Z. L.; Sirianni, D. A.; O’Brien, J. S.; Waldrop, J. M.; Kumar, A.; Hohenstein, E. G.; Pritchard, B. P.; Brooks, B. R.; Schaefer, H. F.; Sokolov, A. Y.; Patkowski, K.; DePrince, A. E.; Bozkaya, U.; King, R. A.; Evangelista, F. A.; Turney, J. M.; Crawford, T. D.; Sherrill, C. D. PSI4 1.4: Open-source software for high-throughput quantum chemistry. *J. Chem. Phys.* **2020**, *152*, 184108.
- (14) Lehtola, S. A review on non-relativistic, fully numerical electronic structure calculations on atoms and diatomic molecules. *Int. J. Quantum Chem.* **2019**, *119*, e25968.
- (15) Becke, A. D. A multicenter numerical integration scheme for polyatomic molecules. *J. Chem. Phys.* **1988**, *88*, 2547–2553.
- (16) te Velde, G.; Bickelhaupt, F. M.; Baerends, E. J.; Fonseca Guerra, C.; van Gisbergen, S. J. A.; Snijders, J. G.; Ziegler, T. Chemistry with ADF. *J. Comput. Chem.* **2001**, *22*, 931–967.
- (17) Ren, X.; Rinke, P.; Blum, V.; Wieferink, J.; Tkatchenko, A.; Sanfilippo, A.; Reuter, K.; Scheffler, M. Resolution-of-identity approach to Hartree–Fock, hybrid density functionals, RPA, MP2 and GW with numeric atom-centered orbital basis functions. *New J. Phys.* **2012**, *14*, 053020.
- (18) Hill, J. G. Gaussian basis sets for molecular applications. *Int. J. Quantum Chem.* **2013**, *113*, 21–34.

- (19) Weigend, F. Accurate Coulomb-fitting basis sets for H to Rn. *Phys. Chem. Chem. Phys.* **2006**, *8*, 1057–65.
- (20) Weigend, F. Hartree–Fock exchange fitting basis sets for H to Rn. *J. Comput. Chem.* **2008**, *29*, 167–175.
- (21) Weigend, F.; Ahlrichs, R. Balanced basis sets of split valence, triple zeta valence and quadruple zeta valence quality for H to Rn: Design and assessment of accuracy. *Phys. Chem. Chem. Phys.* **2005**, *7*, 3297–305.
- (22) Weigend, F.; Köhn, A.; Hättig, C. Efficient use of the correlation consistent basis sets in resolution of the identity MP2 calculations. *J. Chem. Phys.* **2002**, *116*, 3175.
- (23) Hättig, C. Optimization of auxiliary basis sets for RI-MP2 and RI-CC2 calculations: core-valence and quintuple-zeta basis sets for H to Ar and QZVPP basis sets for Li to Kr. *Phys. Chem. Chem. Phys.* **2005**, *7*, 59–66.
- (24) Tanaka, M.; Katouda, M.; Nagase, S. Optimization of RI-MP2 Auxiliary Basis Functions for 6-31G\*\* and 6-311G\*\* Basis Sets for First-, Second-, and Third-Row Elements. *J. Comput. Chem.* **2013**, *34*, 2568–2575.
- (25) Hellweg, A.; Rappoport, D. Development of new auxiliary basis functions of the Karlsruhe segmented contracted basis sets including diffuse basis functions (def2-SVPD, def2-TZVPPD, and def2-QVPPD) for RI-MP2 and RI-CC calculations. *Phys. Chem. Chem. Phys.* **2015**, *17*, 1010–1017.
- (26) Van Lenthe, E.; Baerends, E. J. Optimized Slater-type basis sets for the elements 1-118. *J. Comput. Chem.* **2003**, *24*, 1142–56.
- (27) Chong, D. P.; van Lenthe, E.; Van Gisbergen, S.; Baerends, E. J. Even-tempered Slater-type orbitals revisited: from hydrogen to krypton. *J. Comput. Chem.* **2004**, *25*, 1030–6.

- (28) Manninen, P.; Vaara, J. Systematic Gaussian basis-set limit using completeness-optimized primitive sets. A case for magnetic properties. *J. Comput. Chem.* **2006**, *27*, 434–445.
- (29) Jensen, F. The Basis Set Convergence of Spin-Spin Coupling Constants Calculated by Density Functional Methods. *J. Chem. Theory Comput.* **2006**, *2*, 1360–1369.
- (30) Lehtola, J.; Hakala, M.; Vaara, J.; Hämmäläinen, K. Calculation of isotropic Compton profiles with Gaussian basis sets. *Physical Chemistry Chemical Physics* **2011**, *13*, 5630.
- (31) Lehtola, J.; Manninen, P.; Hakala, M.; Hämmäläinen, K. Completeness-optimized basis sets: Application to ground-state electron momentum densities. *J. Chem. Phys.* **2012**, *137*, 104105.
- (32) Lehtola, S.; Manninen, P.; Hakala, M.; Hämmäläinen, K. Contraction of completeness-optimized basis sets: application to ground-state electron momentum densities. *J. Chem. Phys.* **2013**, *138*, 044109.
- (33) Ambrose, M. A.; Jensen, F. Probing Basis Set Requirements for Calculating Core Ionization and Core Excitation Spectroscopy by the  $\Delta$  Self-Consistent-Field Approach. *J. Chem. Theory Comput.* **2019**, *15*, 325–337.
- (34) Lehtola, S. Polarized Gaussian basis sets from one-electron ions. *J. Chem. Phys.* **2020**, *152*, 134108.
- (35) Yang, R.; Rendell, A. P.; Frisch, M. J. Automatically generated Coulomb fitting basis sets: design and accuracy for systems containing H to Kr. *J. Chem. Phys.* **2007**, *127*, 074102.
- (36) Stoychev, G. L.; Auer, A. A.; Neese, F. Automatic Generation of Auxiliary Basis Sets. *J. Chem. Theory Comput.* **2017**, *13*, 554–562.

- (37) Lehtola, S.; Blockhuys, F.; Van Alsenoy, C. An Overview of Self-Consistent Field Calculations Within Finite Basis Sets. *Molecules* **2020**, *25*, 1218.
- (38) Blum, V.; Gehrke, R.; Hanke, F.; Havu, P.; Havu, V.; Ren, X.; Reuter, K.; Scheffler, M. Ab initio molecular simulations with numeric atom-centered orbitals. *Comput. Phys. Commun.* **2009**, *180*, 2175–2196.
- (39) Ihrig, A. C.; Wieferink, J.; Zhang, I. Y.; Ropo, M.; Ren, X.; Rinke, P.; Scheffler, M.; Blum, V. Accurate localized resolution of identity approach for linear-scaling hybrid density functionals and for many-body perturbation theory. *New J. Phys.* **2015**, *17*, 093020.
- (40) Aquilante, F.; Lindh, R.; Pedersen, T. B. Unbiased auxiliary basis sets for accurate two-electron integral approximations. *J. Chem. Phys.* **2007**, *127*, 114107.
- (41) Aquilante, F.; Gagliardi, L.; Pedersen, T. B.; Lindh, R. Atomic Cholesky decompositions: a route to unbiased auxiliary basis sets for density fitting approximation with tunable accuracy and efficiency. *J. Chem. Phys.* **2009**, *130*, 154107.
- (42) Beebe, N. H. F.; Linderberg, J. Simplifications in the Two-Electron Integral Array in Molecular Calculations. *Int. J. Quant. Chem.* **1977**, *12*, 683–705.
- (43) Boström, J.; Aquilante, F.; Pedersen, T. B.; Lindh, R. Ab Initio Density Fitting: Accuracy Assessment of Auxiliary Basis Sets from Cholesky Decompositions. *J. Chem. Theory Comput.* **2009**, 1545–1553.
- (44) Aquilante, F.; Autschbach, J.; Baiardi, A.; Battaglia, S.; Borin, V. A.; Chibotaru, L. F.; Conti, I.; De Vico, L.; Delcey, M.; Fdez. Galván, I.; Ferré, N.; Freitag, L.; Garavelli, M.; Gong, X.; Knecht, S.; Larsson, E. D.; Lindh, R.; Lundberg, M.; Malmqvist, P. Å.; Nenov, A.; Norell, J.; Odelius, M.; Olivucci, M.; Pedersen, T. B.; Pedraza-González, L.; Phung, Q. M.; Pierloot, K.; Reiher, M.; Schapiro, I.; Segarra-Martí, J.; Segatta, F.;

- Seijo, L.; Sen, S.; Sergentu, D.-C.; Stein, C. J.; Ungur, L.; Vacher, M.; Valentini, A.; Veryazov, V. Modern quantum chemistry with [Open]Molcas. *J. Chem. Phys.* **2020**, *152*, 214117.
- (45) Roland Lindh, private communication, 2021.
- (46) Lehtola, S. Curing basis set overcompleteness with pivoted Cholesky decompositions. *J. Chem. Phys.* **2019**, *151*, 241102.
- (47) Lehtola, S. Accurate reproduction of strongly repulsive interatomic potentials. *Phys. Rev. A* **2020**, *101*, 032504.
- (48) Harbrecht, H.; Peters, M.; Schneider, R. On the low-rank approximation by the pivoted Cholesky decomposition. *Appl. Numer. Math.* **2012**, *62*, 428–440.
- (49) Karton, A.; Sylvetsky, N.; Martin, J. M. L. W4-17: A diverse and high-confidence dataset of atomization energies for benchmarking high-level electronic structure methods. *J. Comput. Chem.* **2017**, *38*, 2063–2075.
- (50) Lehtola, S. Fully numerical Hartree–Fock and density functional calculations. I. Atoms. *Int. J. Quantum Chem.* **2019**, *119*, e25945.
- (51) Higham, N. J. Cholesky factorization. *WIREs Comput. Stat.* **2009**, *1*, 251–254.
- (52) Gerschgorin, S. Über die Abgrenzung der Eigenwerte einer Matrix. *Bull. l’Académie des Sci. l’URSS. Cl. des Sci. mathématiques Nat.* **1931**, 749–754.
- (53) Koch, H.; Sánchez de Merás, A.; Pedersen, T. B. Reduced scaling in electronic structure calculations using Cholesky decompositions. *J. Chem. Phys.* **2003**, *118*, 9481–9484.
- (54) Lehtola, J.; Hakala, M.; Sakko, A.; Hämmäläinen, K. ERKALE – A flexible program package for X-ray properties of atoms and molecules. *J. Comput. Chem.* **2012**, *33*, 1572–1585.

- (55) Lehtola, S. ERKALE – HF/DFT from Hel. 2018; <https://github.com/susilehtola/erkale>.
- (56) Lehtola, S.; Head-Gordon, M.; Jónsson, H. Complex Orbitals, Multiple Local Minima, and Symmetry Breaking in Perdew–Zunger Self-Interaction Corrected Density Functional Theory Calculations. *J. Chem. Theory Comput.* **2016**, *12*, 3195–3207.
- (57) Pritchard, B. P.; Altarawy, D.; Didier, B.; Gibson, T. D.; Windus, T. L. New Basis Set Exchange: An Open, Up-to-Date Resource for the Molecular Sciences Community. *J. Chem. Inf. Model.* **2019**, *59*, 4814–4820.
- (58) Ranasinghe, D. S.; Petersson, G. A. CCSD(T)/CBS atomic and molecular benchmarks for H through Ar. *J. Chem. Phys.* **2013**, *138*, 144104.
- (59) Frisch, M. J.; Trucks, G. W.; Schlegel, H. B.; Scuseria, G. E.; Robb, M. A.; Cheeseman, J. R.; Scalmani, G.; Barone, V.; Mennucci, B.; Petersson, G. A.; Nakatsuji, H.; Caricato, M.; Li, X.; Hratchian, H. P.; Izmaylov, A. F.; Bloino, J.; Zheng, G.; Sonnenberg, J. L.; Hada, M.; Ehara, M.; Toyota, K.; Fukuda, R.; Hasegawa, J.; Ishida, M.; Nakajima, T.; Honda, Y.; Kitao, O.; Nakai, H.; Vreven, T.; Montgomery, J. J. A.; Peralta, J. E.; Ogliaro, F.; Bearpark, M.; Heyd, J. J.; Brothers, E.; Kudin, K. N.; Staroverov, V. N.; Kobayashi, R.; Normand, J.; Raghavachari, K.; Rendell, A.; Burant, J. C.; Iyengar, S. S.; Tomasi, J.; Cossi, M.; Rega, N.; Millam, J. M.; Klene, M.; Knox, J. E.; Cross, J. B.; Bakken, V.; Adamo, C.; Jaramillo, J.; Gomperts, R.; Stratmann, R. E.; Yazyev, O.; Austin, A. J.; Cammi, R.; Pomelli, C.; Ochterski, J. W.; Martin, R. L.; Morokuma, K.; Zakrzewski, V. G.; Voth, G. A.; Salvador, P.; Dannenberg, J. J.; Dapprich, S.; Daniels, A. D.; Farkas, Ö.; Foresman, J. B.; Ortiz, J. V.; Cioslowski, J.; Fox, D. J. Gaussian 09 Revision D.01. 2009.
- (60) Weigend, F.; Furche, F.; Ahlrichs, R. Gaussian basis sets of quadruple zeta valence quality for atoms H–Kr. *J. Chem. Phys.* **2003**, *119*, 12753.

- (61) Hintze, J. L.; Nelson, R. D. Violin Plots: A Box Plot-Density Trace Synergism. *Amer. Statist.* **1998**, *52*, 181–184.
- (62) Lehtola, S.; Karttunen, A. Free and Open Source Software for Computational Chemistry Education. **2021**,
- (63) Miró, P.; Cramer, C. J. Water clusters to nanodrops: a tight-binding density functional study. *Phys. Chem. Chem. Phys.* **2013**, *15*, 1837–1843.
- (64) Head-Gordon, M.; Pople, J. A.; Frisch, M. J. MP2 energy evaluation by direct methods. *Chem. Phys. Lett.* **1988**, *153*, 503–506.
- (65) Csóka, J.; Kállay, M. Speeding up Hartree–Fock and Kohn–Sham calculations with first-order corrections. *J. Chem. Phys.* **2021**, *154*, 164114.
- (66) Aquilante, F.; Pedersen, T. B.; Lindh, R. Low-cost evaluation of the exchange Fock matrix from Cholesky and density fitting representations of the electron repulsion integrals. *J. Chem. Phys.* **2007**, *126*, 194106.
- (67) Herbert, J. M. *Rev. Comput. Chem.*; John Wiley & Sons, Inc., 2015; Vol. 28; pp 391–517.
- (68) Löwdin, P.-O. Quantum theory of cohesive properties of solids. *Adv. Phys.* **1956**, *5*, 1–171.



# Graphical TOC Entry

